Molecular Dynamics Study of a Surfactant-Mediated Decane−Water Interface: Effect of Molecular Architecture of Alkyl Benzene Sulfonate

Seung Soon Jang, Shiang-Tai Lin, Prabal K. Maiti, Mario Blanco, and William A. Goddard III*

Materials and Process Simulation Center, Beckman Institute, California Institute of Technology, Pasadena, California 91125

Patrick Shuler and Yongchun Tang

Power, Energy & Environmental Research Center, California Institute of Technology, Covina, California 91722

Received: March 18, 2004; In Final Form: May 25, 2004

The effect of molecular architecture of a surfactant, particularly the attachment position of benzene sulfonate on the hexadecane backbone, at the decane−water interface was investigated using atomistic MD simulations. We consider a series of surfactant isomers in the family of alkyl benzene sulfonates, denoted by *m*-C16, indicating a benzene sulfonate group attached to the *m*th carbon in a hexadecane backbone. The equilibrated model systems showed a well-defined interface between the decane and water phases. We find that surfactant 4-C16 has a more compact packing, in terms of the interfacial area and molecular alignment at the interface, than other surfactants simulated in this study. Furthermore, surfactant 4-C16 leads to the most stable interface by having the lowest interface formation energy. The interfacial thickness is the largest in the case of surfactant 4-C16, with the thickness decreasing when the benzene sulfonate is located farther from the attachment position of 4-C16 (the 4th carbon). The interfacial tension profile was calculated along the direction perpendicular to the interface using the Kirkwood−Buff theory. From the comparison of the interfacial tension obtained from the interfacial tension profile, we found that surfactant 4-C16 induces the lowest interfacial tension and that the interfacial tension increases with decreasing interfacial thickness as a function of the attachment position of benzene sulfonate. Such a relationship between the interfacial thickness and interfacial tension is rationalized in terms of the miscibility of the alkyl tail of surfactant *m*-C16 with decane by comparing the "effective" length of the alkyl tail with the average end-to-end length of decane. Among the surfactants, the effective length of the 4-C16 alkyl tail (9.53 ± 1.36 Å) was found to be closest to that of decane (9.97 ± 1.03 Å), which is consistent with the results from the density profile and the interfacial tension profile.

1. Introduction

Surfactants are amphiphilic molecules which have one part that is more soluble in water and another part that is more soluble in oil. When added to an oil−water mixture, surfactant molecules are preferentially adsorbed into the interface, leading to a modification of the interfacial properties such as a decrease of interfacial tension. Surfactants are widely employed in household uses such as detergents, food, and cosmetic technology and in large-scale operations in petroleum recovery.[1−4] It is important to understand the underlying principle governing interfacial properties of a given system and, thereby, to design the system or the molecular architecture of surfactants for the purpose of optimizing the performance in which we are interested.

Most thermodynamic models based on the Langmuir adsorption have been developed to describe the equilibrium adsorption of surfactants at the oil−water interface.[5−19] In particular, there have been efforts made to link the given thermodynamic models and molecular information, such as the conformation and intermolecular interaction. Fainerman and co-workers[11,12] have studied the influence of the molecular reorientation of surfactants on the adsorption isotherms by taking into account the conformational dependency of surface area. Blankschtein and co-workers developed a molecular thermodynamic theory for predicting the interfacial behavior of surfactant mixtures that are adsorbed at the air−water[17,18] or the oil−water interface[19] by combining the two-dimensional nonideal gas model[20] with specific molecular properties such as the number of carbons in the surfactant hydrocarbon tail and the molecular cross-sectional area. In these models, knowledge of the molecular structure and interaction is essential for the quantitative prediction and description of the properties of the interface.

Molecular modeling approaches such as the molecular dynamics (MD) and Monte Carlo (MC) simulations have been extensively used for studying the liquid−vapor[21−34] and liquid−liquid[35−51] interfaces. These methods, performed on the basis of the molecular interaction and molecular structures, provide atomistic or molecular details of the interface that are potentially useful for the thermodynamic models mentioned previously. However, among these studies, only a few[40,43,47,49,50] have specifically considered the role of the surfactant at the oil−water interface. Although there have been studies attempting to investigate the dependence of dynamics and morphology of surfactant aggregates on the surfactant structure using coarse-grained modeling techniques,[43,52−56] to our knowledge, there has been no systematic study investigating the effect of

10.1021/jp048773n CCC: $27.50
Published on Web 07/10/2004

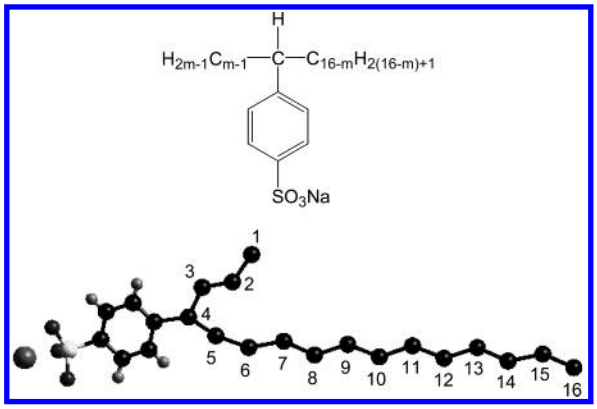

Figure 1. Hexadecane benzene sulfonate surfactant (m = 2, 4, 6, and 8) which has a benzene sulfonate group attached at the mth carbon in the backbone; for convenience, it is denoted as m-C16. The example shown is 4-C16. The benzene sulfonate part adopts the explicit all-atom model and the alkyl part the united atom model.

molecular architecture of surfactants on the interfacial properties, such as interfacial tension and structure, of the oil−water interface.

In this paper, we present a molecular dynamics study on the changes in the decane−water interfacial properties as a function of the structural variable of surfactants. The surfactant molecules used here are a family of hexadecane benzene sulfonate groups denoted by m-C16 (Figure 1), which indicates a benzene sulfonate group attached to the mth carbon in the hexadecane backbone. It was reported previously that the interfacial tension (IFT) between water and decane decreases with the addition of surfactants m-C16 and that the extent of IFT reduction changes with m. The maximum IFT reduction is found with 4-C16.[57] Our goal in this study is to analyze how the variation in the molecular architecture of m-C16 surfactants affects interfacial properties such as the local density profile and IFT of the decane−water interface. For this purpose, we characterized the conformation of surfactants, the density profile, and the interfacial tension profile using surfactants 2-C16, 4-C16, 6-C16, and 8-C16.

2. Model and Simulation Methods

In this simulation, decane was described using the united atom model developed by Smit and co-workers,[58−61] and water using an F3C model.[62] These force fields were extensively tested and also successfully used in our previous studies.[63,64] For the surfactant, the benzene sulfonate part was described by the explicit all-atom model using the Dreiding force field,[65] and the alkyl tail part was described by the same united atom model used for decane. The total potential energy is given as follows:

$$E_{\text{total}} = E_{\text{vdW}} + E_{\text{Q}} + E_{\text{bond}} + E_{\text{angle}} + E_{\text{torsion}} \qquad (1)$$

where E_{total}, E_{vdW}, E_{Q}, E_{bond}, E_{angle}, and E_{torsion} are the total energy and the van der Waals, electrostatic, bond-stretching, angle-bending, and torsion-energy components, respectively. The chemical structures of water, decane, and the surfactants are shown in Figure 2, and their force-field parameters used to calculate the intra- and intermolecular interactions are summarized in Table 1.

For all of the cases (2-C16, 4-C16, 6-C16, and 8-C16), we simulated model systems consisting of the decane and water phases having two decane−water interfaces (Figure 3a), which

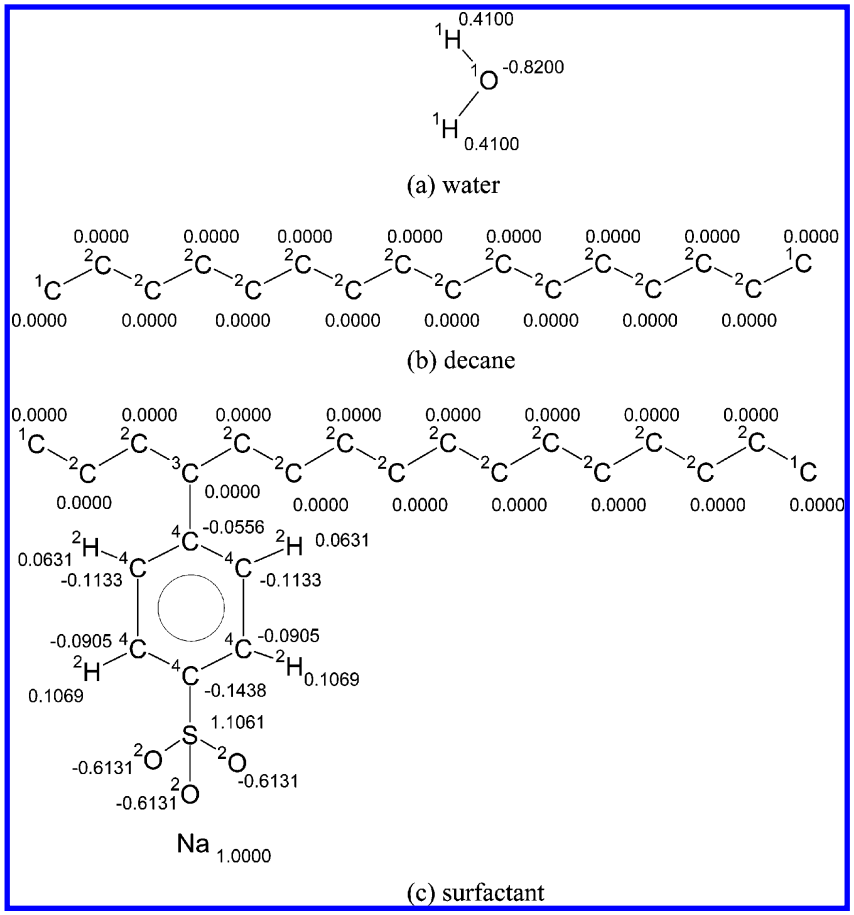

Figure 2. Chemical structure and partial charges of (a) water, (b) decane, and (c) surfactant (4-C16). The superscripts to the left and above the atoms denote the atom types used in Table 1.

TABLE 1: Force-Field Parameters Used for the Decane−Water Interface with a Surfactant

$$E_{\mathrm{vdW}}(R) = D_0\left\{\left(\frac{R_0}{R}\right)^{12} - 2\left(\frac{R_0}{R}\right)^{6}\right\},\ E_{\mathrm{Q}}{}^{a} = 322.0637\sum_{i>j}\frac{Q_i Q_j}{\epsilon R_{ij}}$$

$$E_{\mathrm{bond}}(R) = \frac{1}{2}K_{\mathrm{b}}(R - R_0)^2,\ E_{\mathrm{angle}}(\theta) = \frac{1}{2}K_{\theta}(\theta - \theta_0)^2$$

$$E_{\mathrm{torsion}}(\phi) = \sum_n \frac{1}{2}V_n[1 - d_n\cos(n\phi)]$$

E_{vdW}	^{1}H(HF3C)	$R_0{}^b$	0.9000	$D_0{}^c$	0.0100		
	^{1}O(OF3C)	R_0	3.5532	D_0	0.1848		
	^{1}C(C_33)	R_0	4.4113	D_0	0.2265		
	^{2}C(C_32)	R_0	4.4113	D_0	0.0934		
	^{3}C(C_31)	R_0	3.3953	D_0	0.0934		
	^{4}C(C_R)	R_0	3.8983	D_0	0.0951		
	^{2}H(H_)	R_0	3.1950	D_0	0.0152		
	S(S_3)	R_0	4.0300	D_0	0.3440		
	^{2}O(O_2)	R_0	3.4046	D_0	0.0957		
	Na	R_0	3.1440	D_0	0.5000		
E_{bond}	OF3C−HF3C	R_0	1.0000	$K_{\mathrm{b}}{}^d$	500.0000		
	C_33−C_32	R_0	1.5400	K_{b}	520.0000		
	C_32−C_32	R_0	1.5400	K_{b}	520.0000		
	C_31−C_33	R_0	1.5400	K_{b}	520.0000		
	C_31−C_32	R_0	1.5400	K_{b}	520.0000		
	C_31−C_R	R_0	1.4600	K_{b}	700.0000		
	C_R−C_R	R_0	1.3900	K_{b}	1050.0000		
	C_R−H_	R_0	1.0200	K_{b}	700.0000		
	S_3−O_2	R_0	1.4800	K_{b}	700.0000		
E_{angle}	HF3C−OF3C−HF3C	$\theta_0{}^e$	109.4700	$K_\theta{}^f$	120.0000		
	C_33−C_32−C_32	θ_0	114.0000	K_θ	124.1900		
	C_32−C_32−C_32	θ_0	114.0000	K_θ	124.1900		
	C_33−C_31−C_32	θ_0	114.0000	K_θ	124.1900		
	C_33−C_32−C_31	θ_0	114.0000	K_θ	124.1900		
	C_32−C_31−C_32	θ_0	114.0000	K_θ	124.1900		
	C_33−C_31−C_R	θ_0	109.4710	K_θ	100.0000		
	X−C_R−X	θ_0	109.4710	K_θ	100.0000		
	O_2−S_3−O_2	θ_0	115.5000	K_θ	350.0000		
E_{torsion}	X−C_32−C_32−X	V_1 (d_1)^g	1.4109 (−1)	V_2 (d_2)	−0.271 (1)	V_3 (d_3)	2.787 (−1)
	X−C_31−C_32−X	V_1 (d_1)	1.4109 (−1)	V_2 (d_2)	−0.271 (1)	V_3 (d_3)	2.787 (−1)
	X−C_31−C_R−C_R	V_6 (d_6)	1.0000 (1)				
	X−S_3−C_R−X	V_2 (d_2)	2.0000 (1)				

[a] Q_i and Q_j are atomic charge of atoms i and j, respectively. Except for water, all atomic charges were calculated from QM Mulliken populations at the level of 6-31G**/B3LYP. The atomic charges for water molecules and for decane are from the F3C model in ref 62 and from the united atom model of hydrocarbon in refs 58−61, respectively. [b] Å for R_0. [c] kcal/mol for D_0. [d] kcal mol^{-1} Å^{-2} for K_{b}. [e] Deg for θ_0. [f] kcal mol^{-1} deg^{-2} for K_θ. [g] kcal/mol for V_n.

have been widely used for the studies of liquid−liquid interfaces.[35,39,42,44,50,51] All of the systems have the same composition: 120 decane molecules, 800 water molecules, and 32 surfactants. To construct this configuration, first, we prepared the monolayer consisting of 16 surfactants on an assumption of hexagonal closed packing in an orthorhombic simulation box with the periodic boundary condition applied to all three spatial directions (Figure 3b). Then, we carried out an energy minimization to relax this monolayer of surfactants with the fixed-cell dimensions (L_x, L_y, and L_z). The next step was to prepare the decane and water phases separately using NVT MD simulations based on the experimental densities (at 300 K and 1 atm, 0.725 g/cm^3 for decane[66−69] and 0.997 g/cm^3 for water[70−72]). The cell parameters of the simulation box were set to have the same L_x and L_y dimensions as the orthorhombic simulation box with the surfactant monolayer. As the final step, we integrated these three phases into one simulation box. Before applying MD simulation to equilibrate this integrated system, we performed an energy minimization to relax the system during which the cell parameters L_x, L_y, and L_z of the orthorhombic simulation box were adjusted to obtain better interaction between the newly jointed phases. Once the initial system was prepared, NVT and NPT MD simulations were sequentially carried out to equilibrate the system. First, a NVT MD simulation was performed for 200 ps at 300 K as a pretreatment for overcoming local minima by imposing thermal energy in a constant volume condition. Then, a final equilibration was done by a NPT MD simulation for 400 ps at 300 K and 1 atm to adjust the system to a more realistic density. To obtain good statistics, we simulated two independent samples for each surfactant case (from 2-C16 to 8-C16) with the NPT MD simulation for 2 ns at 300 K and 1 atm. In addition, we prepared the bare decane−water interface consisting of 120 decane molecules and 800 water molecules without surfactants as a reference for comparison. Here, the kind of concentration with which our simulations are working should be addressed. From the general consensus saying that surfactant concentration at the interface is a function of the concentration in the bulk phase below the CMC (critical micelle concentration) but saturated above the CMC, it seems to be clear that we are dealing with a case in which the bulk concentration is above the CMC, although the finite system size of our simulation does not allow free surfactant in the bulk phases. Therefore, the surfactant concentration and the interfacial properties in our simulations are insensitive to the variation in the bulk phase.

Throughout this study, all MD simulations were performed with the LAMMPS (large-scale atomic/molecular massively parallel simulator) code from Plimpton at Sandia (modified to handle our force fields).[73,74] The equations of motion were integrated using the Verlet algorithm[75] with a time step of 1.0

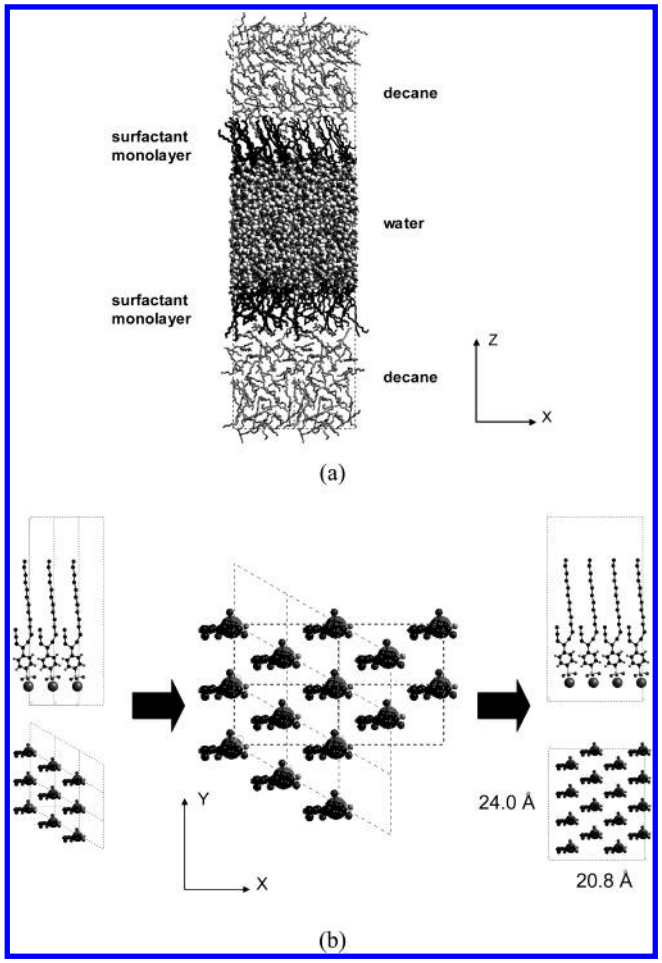

Figure 3. Simulated configuration of the decane−water interface in the presence of a surfactant monolayer (a) and the initial hexagonal packing of the surfactant monolayer (b).

fs. A Nose−Hoover-type thermostat[76−78] with a relaxation time of 0.1 ps was used to control the temperature, and the pressure was controlled isotropically.[79] The Lennard-Jones potential parameters for the van der Waals interaction of heterogeneous atomic pairs were calculated from the geometric mean of parameters of each atom. The particle−particle particle−mesh Ewald (PPPM) method[80] (accuracy criterion was set to 1.0×10^{-5} and the near-field cutoff to 15.0 Å) was used for the long-range correction of electrostatic interactions.

3. Results and Discussion

3.1. Equilibrated System: Surfactant Conformation and Interface Formation Energy. Figure 3a illustrates a snapshot of the equilibrated structure of the decane−4-C16−water system after a 400 ps equilibration. The volumetric properties were converged from the equilibration since the volume fluctuation from a subsequent 2 ns NPT MD simulation for data collection is less than 1% of the average value. The structures of the other cases are quite similar, and the fluctuations of the cell in each dimension are summarized in Table 2. A point of interest is that surfactant 4-C16 has the smallest interfacial area ($L_x \times L_y$), and this area increases when the benzene sulfonate is attached to a position farther from the 4th carbon, which correlates with the lowest IFT value for the decane−water interface using surfactant 4-C16.

To characterize the conformations of surfactants at the interface, we calculated the principal moments of inertia of each individual surfactant and the tilt angle between the largest principal moment and the interface normal vector. The results listed in Table 3 are averaged values from the equilibrated 2 ns MD trajectories. A common feature in all of the cases is that the surfactant molecules are packed like cylinders (having one long principal axis of moment of inertia, I_3, and two smaller, similar valued ones, I_1 and I_2) with a tilt angle ranging over 20−27°. It should be noted, however, that surfactant 4-C16 has the largest $I_3/I_{1,2}$ ratio and the smallest tilt angle, indicating that 4-C16 surfactants are aligned more vertically with the smaller molecular cross-sectional area at the interface, while the other surfactants have a 2-dimensionally dispersed conformation with a larger cross-sectional area. This is consistent with the results of the interfacial area in Table 2. From these results, we conclude that 4-C16 has more compact packing than the other cases have at the decane−water interface.

Next, to compare the energetic stability of each system, we calculated the interface formation energy (IFE) defined as follows:

$$\mathrm{IFE} = \frac{E_{\mathrm{total}} - (nE_{\mathrm{surfactant,single}} + E_{\mathrm{decane-water}})}{n} \qquad (2)$$

where E_{total}, $E_{\mathrm{surfactant,single}}$, and $E_{\mathrm{decane-water}}$ denote the energies of whole system, the single surfactant molecule that is calculated from a separate 100 ps MD simulation in vacuum at the same temperature, and a bare decane−water system, respectively. The variable n is the number of surfactant molecules (32 in this study). The value of IFE is a measure of the average intermolecular interaction per surfactant molecule arising from the insertion of one surfactant molecule into the decane−water interface. The components necessary for this calculation and the results are summarized in Table 4. Although each surfactant has almost the same value for the single molecular energy ($E_{\mathrm{surfactant,single}}$), 4-C16 has the lowest E_{total} and thereby the lowest IFE, implying that the 4-C16-mediated interface is the most stable in terms of energetics. The results also show that molecular interactions between surfactants themselves and between surfactants and solvents are affected by the surfactant molecular architecture.

3.2. Density Profiles. Figure 4 shows the density profiles of each system along the *z*-axis direction of the simulation box, which were obtained by dividing the system into 1.5 Å thick slabs parallel to the *xy* plane. From the density profile, it is clear that the system consists of two phases (invariant density with *z*) with two well-defined interfaces (varying density with *z*). It should be noted here that the densities of each phase in the decane−surfactant−water system (0.723 ± 0.005 for decane and 0.994 ± 0.005 for water) agree well with those of the pure bulk phase (0.725 g/cm^3 for decane[66−69] and 0.997 g/cm^3 for water[70−72]). This shows that our simulation is sufficiently large for studying a realistic interface between two bulk phases. Another noteworthy point in Figure 4 is that most of the sodium ions stay between the water and the surfactant monolayer (within the average distance of ∼4.0 Å from the sulfur atoms) during a 2 ns MD simulation. The binding of a counterion to an ionic surfactant at the interface has been well-characterized over a wide range of surfactant concentrations, especially above the CMC in experiment[81] as well as theory.[9] Thus, we believe that such a distribution of sodium ions in our simulation in the absence of a background salt concentration is in good agreement with the previous studies.

On the basis of this density profile, we calculated the interfacial thickness between decane and water. As shown in Figure 5, the density profile obtained from our simulation was fitted using the following hyperbolic tangent function that has

TABLE 2: Equilibrated Cell Parameters of the Simulation Box[a]

system	L_x (Å)	L_y (Å)	L_z (Å)	area/molecule (Å^2)	density (g/cm^3)
decane−water	28.90 ± 0.08	28.90 ± 0.08	77.27 ± 0.22		0.81 ± 0.01
2-C16	21.96 ± 0.05	28.72 ± 0.07	133.55 ± 0.31	39.42 ± 0.13	0.88 ± 0.01
4-C16	21.86 ± 0.06	26.72 ± 0.07	143.95 ± 0.18	36.51 ± 0.13	0.88 ± 0.01
6-C16	21.93 ± 0.05	29.51 ± 0.07	131.10 ± 0.31	40.45 ± 0.13	0.87 ± 0.01
8-C16	26.91 ± 0.05	34.89 ± 0.07	90.05 ± 0.18	58.68 ± 0.17	0.87 ± 0.01

[a] During NPT MD simulation, the shape of the simulation box was retained as orthorhombic.

TABLE 3: Principal Axis Lengths of the Moment of Inertia for Surfactant Molecules and the Tilt Angle of the Longest Principal Axis to the Normal Vector to the Planar Interface

surfactant	$I_{1,2} = (I_1 + I_2)/2$ (Å)	I_3 (Å)	$I_3/I_{1,2}$	tilt angle (deg)
2-C16	1.61 ± 0.60	5.50 ± 0.56	3.42 ± 1.32	27.02 ± 11.78
4-C16	1.27 ± 0.53	5.90 ± 0.54	4.64 ± 1.96	20.16 ± 9.45
6-C16	1.55 ± 0.78	4.99 ± 0.46	3.23 ± 1.66	20.20 ± 9.92
8-C16	2.04 ± 1.21	3.93 ± 0.52	1.93 ± 1.18	26.31 ± 11.93

TABLE 4: Interface Formation Energy

system	E_{total} (kcal/mol)	$E_{surfactant,single}$ (kcal/mol)	IFE (kcal/mol)
2-C16	−13341.01 ± 66.04	−92.66 ± 4.25	−73.909 ± 0.004
4-C16	−13355.22 ± 74.57	−92.44 ± 4.06	−74.573 ± 0.004
6-C16	−13338.12 ± 64.25	−93.09 ± 4.42	−73.388 ± 0.004
8-C16	−13045.97 ± 70.53	−92.61 ± 4.23	−64.739 ± 0.003
$E_{decane-water}$		−8010.81 ± 62.37	

been used for the liquid−vapor interface.[51,82−85]

$$\rho_i(z) = 0.5\rho_{i,bulk} - 0.5\rho_{i,bulk}\tanh\left(\frac{2(z - z_0)}{d}\right) \qquad (3)$$

where ρ_i is the density, z_0 is the position of the Gibbs dividing surface, and d is the adjustable parameter related to the interfacial thickness. A common practice for defining the interfacial thickness for the liquid−vapor interface is the "10−90" criterion,[51,82,84,85] which defines the interfacial thickness to be the distance between two positions where the density varies from 10 to 90% of the density of the bulk phase. However, defining the thickness for a complicated interface such as the oil−water interface in the presence of a surfactant is not a trivial matter. Although the density profiles of the oil−surfactant−water interfaces shown in Figure 5 suggest the consideration of two subinterfaces (one between water and the surfactant and the other between the surfactant and oil), the bulk density of the surfactant layer (normally monolayer) is not defined, so it is ambiguous to characterize these two subinterfaces. Thus, we suggest a "90−90" interfacial thickness (t_{total}) criterion, which is the distance between two positions where the densities of decane and water are 90% of their own bulk densities. Figure 5 illustrates this idea. The interfacial thickness consists of the three components t_{oil}, t_{water}, and $t_{surfactant}$: t_{oil} and t_{water} are defined as the 10−90 thickness of the decane and water phases, respectively, and $t_{surfactant}$ is calculated as $t_{surfactant} = t_{total} - (t_{oil} + t_{water})$. Thus, the bare decane−water interface does not have $t_{surfactant}$.

The results of the interfacial thickness analysis are summarized in Table 5. For the bare decane−water interface (in the absence of a surfactant), we determined the interfacial thickness to be 3.90 Å, which is in good agreement with the measured thickness (4.6 ± 0.2 Å) observed from the synchrotron X-ray reflectivity experiment,[86] the prediction from the capillary-wave theory (3.41 Å),[86] and the other MD simulation results (1.99 Å).[51] From the results in Table 5 as well as Figures 4 and 5, it is clear that the interfaces of components t_{oil} and t_{water} are broadened with the addition of a surfactant because decane and water penetrate into hydrophobic alkyl tails and hydrophilic sulfonate groups, respectively. Interestingly, this interface broadening occurred mainly in the decane side and is strongly dependent on the attachment position of benzene sulfonate in the hexadecane backbone, whereas the water interface was insensitive to the variation of the attachment position. This is attributed to the fact that, while all of the surfactants have the same polar group (benzene sulfonate), the different attachment positions in the backbone give rise to the different effective alkyl tail lengths, which may affect the intermolecular interaction with decane molecules. It is important to note that the interfacial thickness (Table 5) does not vary monotonically as a function of the attachment position: surfactant 4-C16 results in the maximum broadening of the interface of the decane side (t_{oil}), implying that the alkyl tail part of surfactant 4-C16 has the best miscibility with decane among the other surfactants. Interestingly, it is observed that 4-C16 induces the thickest interface for both t_{total} and $t_{surfactant}$. This can be explained by considering the packing and conformation of surfactant molecules at the interface as mentioned in section 3.1. In Table 2, it is shown that 4-C16 has the smallest interfacial area ($L_x \times L_y$) and the most extended conformation, which clearly shows that it has the most compact packing at the interface.

On the basis of this definition of the interface and its thickness, the conformation of the alkyl tail of the surfactant as well as that of decane was characterized by investigating their torsion angles. In Figure 6, we present the ratio of trans to gauche for the torsion angle in the alkyl tail of the surfactant and decane. Note, surfactant 4-C16 has the largest trans/gauche ratio among the cases, indicating that the conformation of the alkyl tail of 4-C16 is more extended than that of the other surfactants. Again, this result is consistent with our previous analysis, concluding that 4-C16 has more compact packing with a small tilt angle and small cross-sectional area. In addition, it is clearly noticeable in Figure 6 that the value of the trans/gauche ratio of the decane at the interface where the decane phase contacts the surfactant molecules is larger than that of decane belonging to its bulk phase. In particular, it is observed that 4-C16 has the largest ratio for the decane at the interface, and the trans/gauche ratio for the decane at the interface as a function of surfactant architecture is very similar to that for the alkyl tail of the surfactant. It is thought, therefore, that a larger trans/gauche ratio for the decane at the interface rather than at the bulk phase is induced by the conformation of an alkyl tail of the surfactant since the interface is a coexisting phase where the decane molecules are mixed with the surfactants. We infer that the largest ratio for the decane at the interface in the case of 4-C16 also indicates that the 4-C16 surfactant has better miscibility than the other surfactants.

3.3. Interfacial Tension. We calculated the interfacial tension (γ) in our surfactant-mediated decane−water interface normal to the z-axis using its mechanical definition[87,88]

$$\gamma = \frac{1}{2}\int_0^{L_z} dz[P_N(z) - P_T(z)] \qquad (4)$$

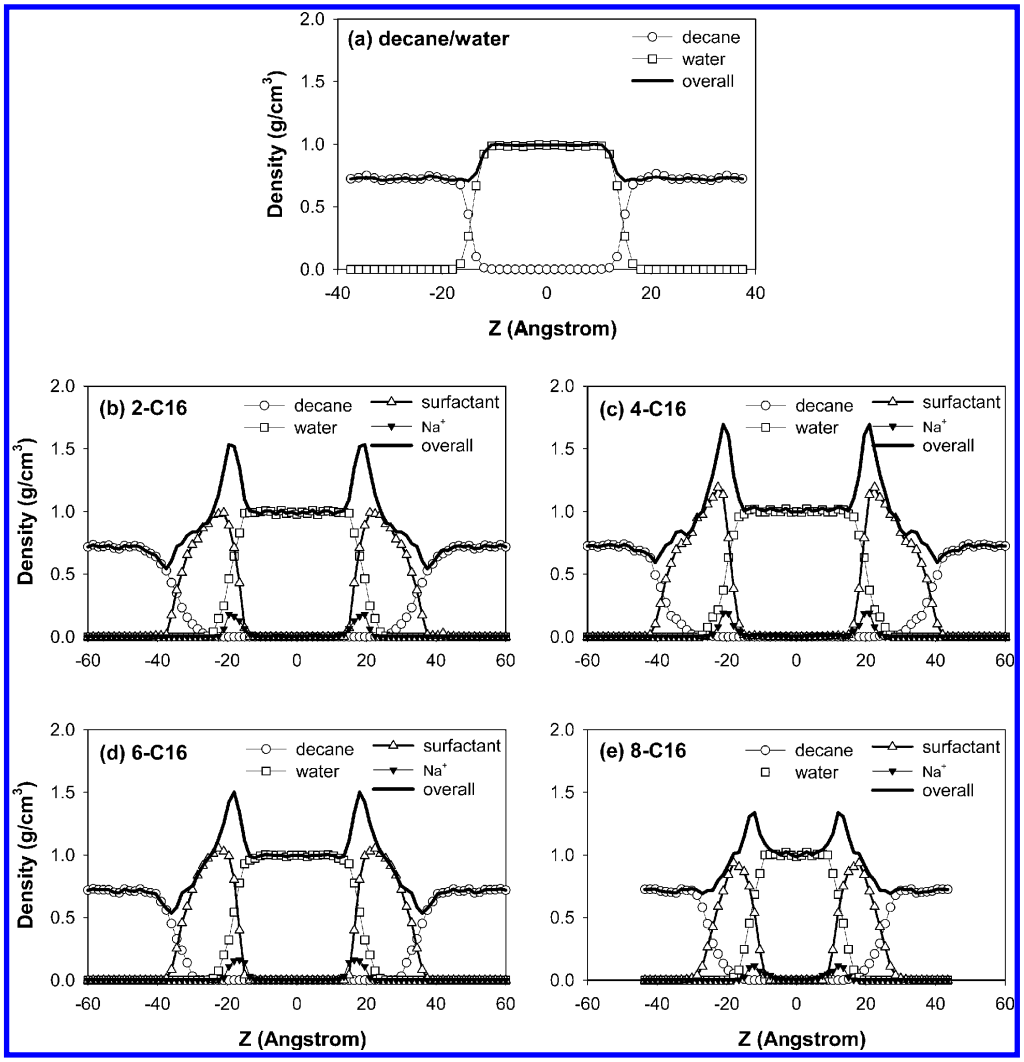

Figure 4. Density profiles along the *z*-axis direction.

where P_N and P_T are the normal and tangential components of the pressure with respect to the planar interface, respectively. P_N and P_T are the same in the bulk phase because the structure is isotropic in any direction, and they are different from each other only near the interface because the structure can be very anisotropic (e.g., Figures 3 and 4). P_N and P_T were calculated from each slab of the simulation box during the simulation as a time average by the Kirkwood−Buff theory[89] that has been successfully used for liquid−vapor[21,23−25,61,82−84,90] and liquid−liquid[35,37,38,40,42,44,47,50,51] interfaces.

$$P_N(z) = \rho(z)k_BT - \frac{1}{V_{slab}}\left\langle \sum_{i,j} \frac{z_{ij}^2}{r_{ij}} \frac{du(r_{ij})}{dr_{ij}} \right\rangle \quad (5)$$

$$P_T(z) = \rho(z)k_BT - \frac{1}{V_{slab}}\left\langle \sum_{i,j} \frac{x_{ij}^2 + y_{ij}^2}{2r_{ij}} \frac{du(r_{ij})}{dr_{ij}} \right\rangle \quad (6)$$

where $\rho(z)$ denotes the density of the slab at z and V_{slab} denotes the slab volume. k_B and T are the Boltzmann constant and the absolute temperature, respectively. Angle brackets represent an ensemble average of all atoms located in the slab at z. r_{ij}, x_{ij}, y_{ij}, and z_{ij} are the distances between the atoms and its components, and $u(r_{ij})$ is the potential energy of the atomic pair i and j. If atom i belongs to the slab z_1, the virial contribution of i is added to the P_N (z_1) or P_T (z_1). Similarly, the virial contribution of j is added to the virial sum of slab z_2 to which atom j belongs.

Figure 7 shows the equilibrated behavior of the interfacial tension as a function of simulation time for the typical case of surfactant 4-C16. The interfacial tension profiles for the systems studied here are shown in Figure 8. Compared to the interfacial tension profile of the decane−water interface (Figure 8a) which shows a single peak, there are two distinct peaks at the interface (panels b−e of Figure 8) with the presence of surfactant molecules. This indicates that two kinds of subinterfaces exist at the molecular level: one is between oil and the surfactant and the other is between the surfactant and water, as observed in the density profile analysis above. At positions far from the interface, the bulk phase has an interfacial tension value of zero on average. These two peaks are located within the 90−90 interface (between the dashed line and the solid line), determined from the density profile. Furthermore, surfactant 4-C16 has the greatest distance between these two peaks (∼7.5 Å) compared with the other cases (∼4.5 Å), which is similar to the feature of $t_{surfactant}$ (Table 5). From these results, we believe that the interfacial tension description of the interface with a surfactant is consistent with that of the 90−90 interface from the density profile.

By integrating these profiles, we obtained the interfacial tensions (Table 6). First, to validate our calculation of the interfacial tension, we simulated the water−vacuum and the decane−vacuum interfaces which consist of the same number

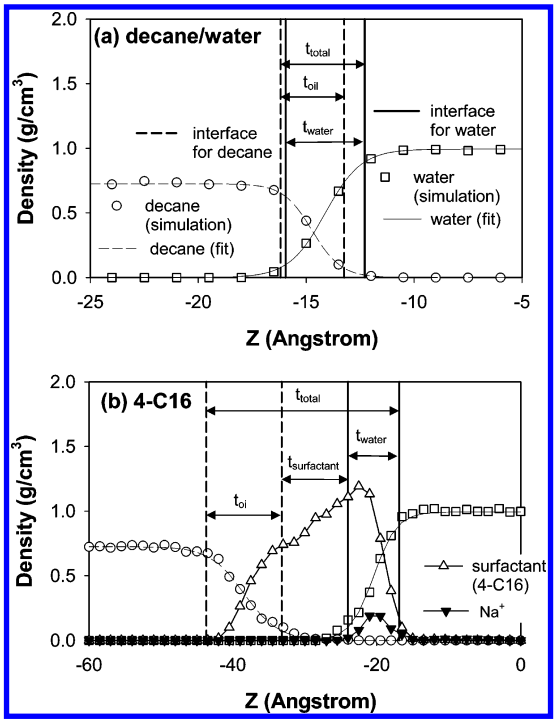

Figure 5. Definition of interfacial thickness.

TABLE 5: Interfacial Thickness

system		z_0 (Å)	d (Å)	t_i (Å)[a]	$t_{surfactant}$[b] (Å)	t_{total} (Å)
decane−water	decane	±14.71	1.34	2.94		3.90
	water	±14.12	1.67	3.67		
2-C16	decane	±34.96	4.63	10.18	6.73	23.98
	water	±19.23	3.22	7.07		
4-C16	decane	±38.45	4.76	10.47	9.20	26.80
	water	±20.44	3.25	7.13		
6-C16	decane	±34.86	4.19	9.21	8.34	24.48
	water	±18.45	3.15	6.93		
8-C16	decane	±24.35	3.95	8.69	3.35	18.83
	water	±13.26	3.09	6.79		

[a] i = oil or water. [b] $t_{surfactant} = t_{total} - (t_{oil} + t_{water})$.

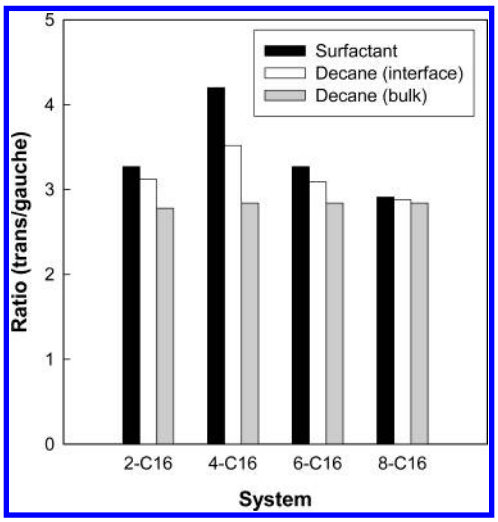

Figure 6. Trans/gauche ratio of the alkyl tail of a surfactant, decane at interface, and decane in bulk phase.

of water or decane molecules as used in each phase of the decane−water and decane−surfactant−water interfaces. The calculated interfacial tension at 300 K was 21.77 ± 2.31 dyn/cm for the decane−vacuum interface and 70.94 ± 2.25 dyn/cm for the water−vacuum interface, which agree very well with

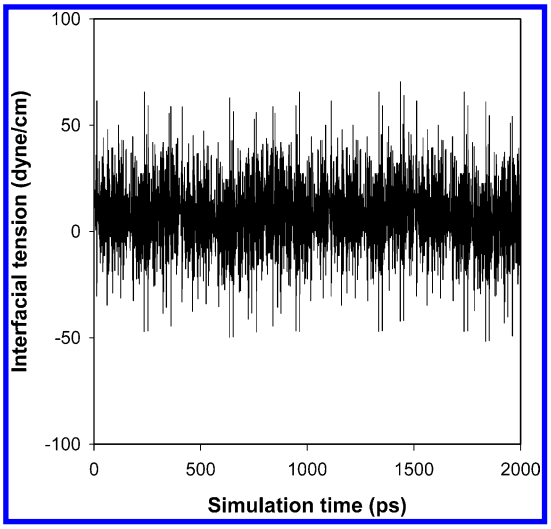

Figure 7. Typical equilibrated behavior of the interfacial tension as a function of the simulation time for the case of surfactant 4-C16.

the experimental values (23.20 dyn/cm for the decane[91] and 71.72 dyn/cm for the water[72,92]). In addition, the interfacial tension of the decane−water interface without a surfactant was 54.70 ± 3.62 dyn/cm, which is also in good agreement with the experimental value (51.72 dyn/cm).[93] Please note that these values were obtained without adjusting the given force fields (the united atom force field[58−61] for decane and the F3C force field[62] for water). We believe that our calculated results for the interfacial tension imply that the current force field provides acceptable accuracy for describing the interfacial systems in which we are interested. Figure 9 shows the comparison of the interfacial tension calculated from our simulations with the experimental values[57] in which we found a qualitative agreement: the interfacial tension of the surfactant-mediated decane−water interface is changed as a function of the attachment position of the benzene sulfonate group, and the lowest interfacial tension is observed in the surfactant 4-C16 case. It should be addressed, however, that the interfacial tension reported from the experiment was measured in the presence of 2 wt % isopentanol as a cosurfactant and 0.003 g/cm^3 of NaCl, which is generally known to have the effect of lowering the interfacial tension of the system dramatically. As the effect of other components such as cosurfactants and salt is out of the scope of this study, we focus on capturing the trend of the interfacial tension along the molecular architectural variation of the surfactant.

3.4. Effective Alkyl Tail Length. The consistent results from the analysis of the density profile and the interfacial tension profile indicate that the decane−water interface in the presence or absence of a surfactant was successfully described in our simulation. Nonetheless, one important question still remains to be answered: why does the 4-C16 surfactant result in the lowest interfacial tension among other surfactants? As a first step toward answering this question, we find that the 4-C16 surfactant induces the maximum interfacial thickness broadening compared to the other surfactants. This interesting feature is summarized in Figure 10, showing that there is strong correlation between the interfacial thickness and the interfacial tension. Since all the surfactants have the same architecture of benzene sulfonate as a polar pendant group, we may infer that the maximum broadening (between decane and the alkyl tail (t_{oil}) and, thereby, between decane and water (t_{total})) induced by 4-C16 is a result of the better miscibility of the alkyl tail of 4-C16 with decane compared to other surfactants. In this situation, the

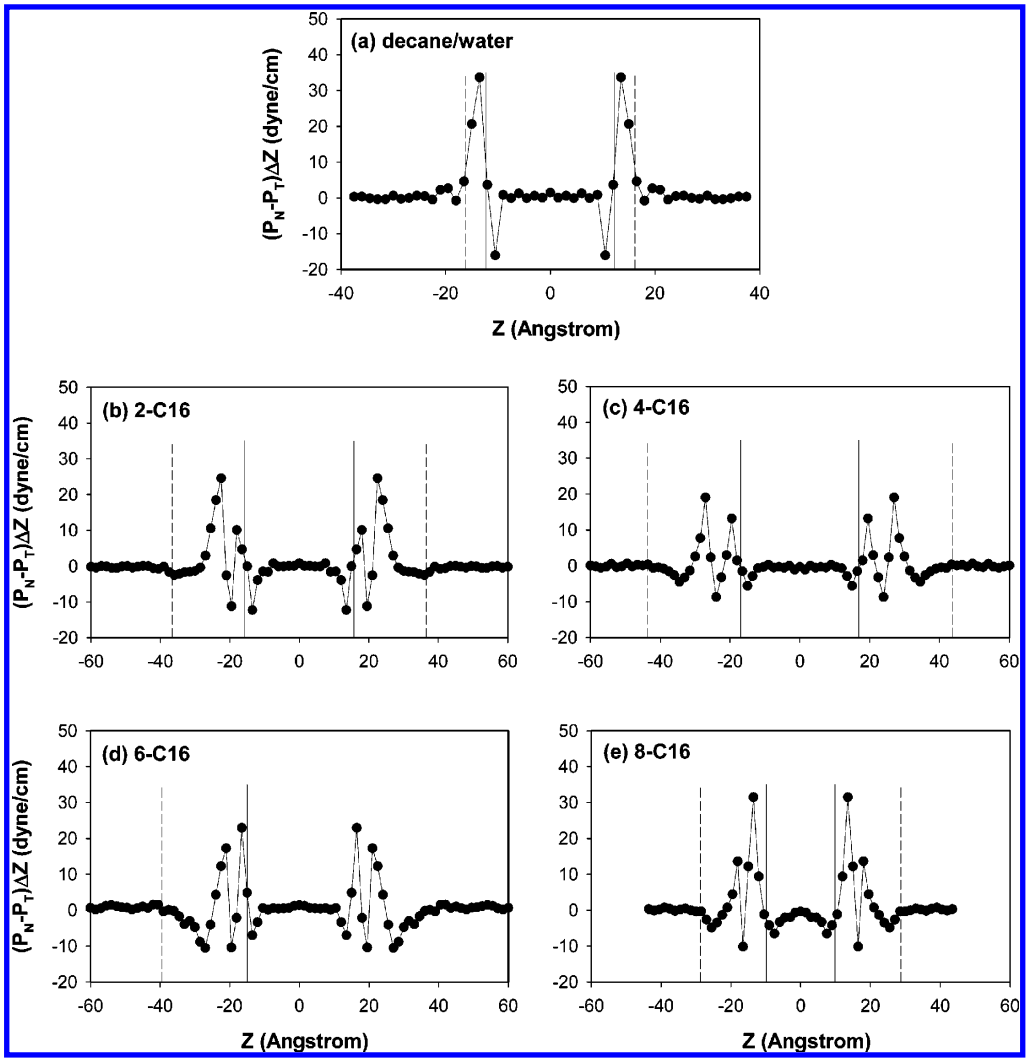

Figure 8. Interfacial tension profile along the *z*-axis direction. The dashed and solid lines indicate the 90−90 interface defined by the two positions ranging from 90% of decane bulk density to 90% of water bulk density.

TABLE 6: Interfacial Tension

	interfacial tension (dyn/cm)[a]	
system	simulation	experiments
decane	21.77 ± 2.31	23.20[b]
water	70.94 ± 2.25	71.71[c]
decane−water	54.70 ± 3.62	51.72[d]
2-C16	23.19 ± 4.94	
4-C16	8.02 ± 4.12	
6-C16	18.12 ± 4.39	
8-C16	30.21 ± 4.41	

[a] The standard deviations were calculated from the average values of five 400 ps-long trajectories. [b] From ref 91. [c] From refs 72 and 92. [d] From ref 93.

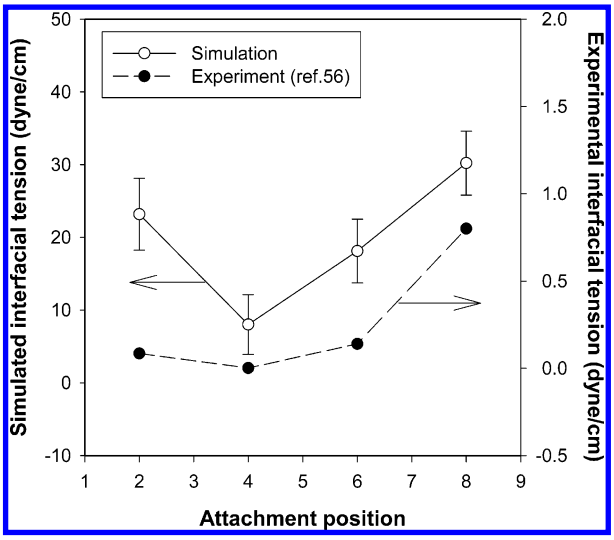

Figure 9. Comparison of interfacial tension between our simulation and the experiment (ref 56).

better miscibility of 4-C16 (with decane at the interface) does not seem to be explained only by the intermolecular interaction (since all of the surfactants have the same kind of alkyl moiety as the decane does), and the only difference among the surfactants, from 2-C16 to 8-C16, is the attachment position of the benzene sulfonate group. Instead, the more plausible explanation is to consider the size similarity of surfactant with decane, which was inspired by the simple idea that decane has better miscibility with itself than it does with any other alkane homologues such as hexane, octane, and so forth.

For this purpose, first, we defined the alkyl tail length as the distance between the backbone ends and the carbon on which the benzene sulfonate group is attached. For each surfactant molecule, there are two tail lengths in one surfactant molecule: one is r_{long}, and the other is r_{short}, as shown in Figure 11. The different attachment position gives rise to the different alkyl tail lengths (e.g., 2-C16 has two asymmetric tails, whereas 8-C16

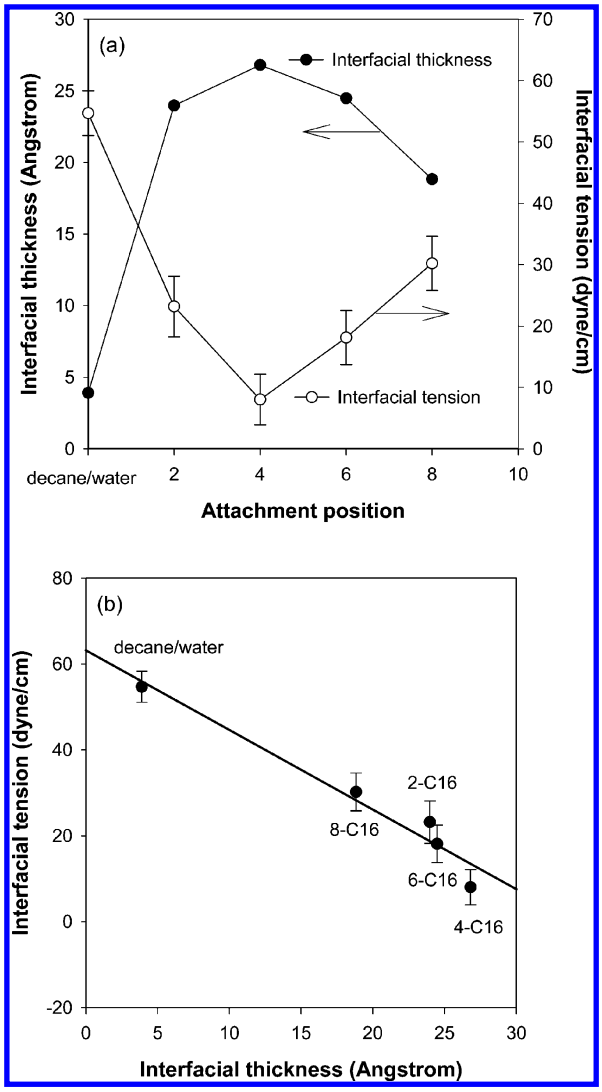

Figure 10. Relationship between the interfacial thickness and the interfacial tension. The solid line in (b) is the least-squares fit of the given results.

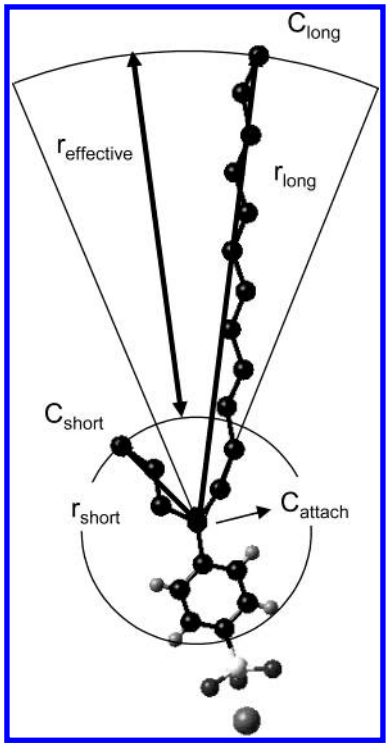

Figure 11. Effective length of the alkyl tail ($r_{effective}$) of the surfactant that is defined as the difference between the average length of the long tail (r_{long}) and that of the short tail (r_{short}).

TABLE 7: Alkyl Tail Length of the Surfactant

system	end-to-end length (Å)		
decane	9.97 ± 1.03		
	r_{long} (Å)	r_{short} (Å)	$r_{effective}$ (=r_{long} − r_{short}) (Å)
2-C16	14.79 ± 1.43	1.54 ± 0.03	13.25 ± 1.43
4-C16	13.37 ± 1.35	3.84 ± 0.19	9.53 ± 1.36
6-C16	10.92 ± 0.96	5.75 ± 0.46	5.17 ± 1.07
8-C16	8.97 ± 0.76	8.01 ± 0.60	0.96 ± 0.97

has almost symmetric ones). Next, we define the "effective" length (Figure 11) to be the difference between r_{long} and r_{short}. This is because the effective tail length of the surfactant which contacts the decane molecules may not be necessarily the same as r_{long} or r_{short}. In other words, in the surfactant layer at the interface, a certain space of longer alkyl tails close to the attachment point (C_{attach} in Figure 11) may not be accessible due to the steric hindrance from the shorter tail. Therefore, the effective tail length ($r_{effective}$) is closer to the true length of the alkyl tail that is accessible for decane (solvent) although its degree of freedom is not completely the same as the free alkane molecule.

Table 7 summarizes the statistical values of the alkyl tail lengths. It should be mentioned that for the case of 8-C16 which has nearly symmetric tail lengths, r_{long} and r_{short} are suitable for comparison with other cases because the two tails have similar length and neither of them has a dominant role for mixing with decane. Remarkably, $r_{effective}$ of surfactant 4-C16 is almost the same as the end-to-end length of decane, and all of the other lengths are farther from the length of decane. We believe that this argument rationalizes the reason that surfactant 4-C16 has the lowest interfacial tension and the largest interfacial thickness. This argument seems to be related to the influence of the alkyl tail length on the mixing entropy at the interface, and we leave its quantitative assessment for future study.

4. Summary

Using MD simulations, we studied the effect of molecular architecture of a surfactant at the decane−water interface as a function of the attachment position of benzene sulfonate on the hexadecane backbone. For this purpose, we prepared the equilibrated model systems which consist of decane, water bulk phases, plus a surfactant layer at the interface.

The system with surfactant 4-C16 is found to have the smallest interfacial area ($L_x \times L_y$) compared with the other surfactants, and the equilibrated molecular conformation of 4-C16 was aligned more vertically with the largest ratio of principal axis length of moments of inertia ($I_3/I_{1,2}$). These results show that 4-C16 has more compact packing at the decane−water interface than do the other cases. The interface formation energy was the lowest for the 4-C16-mediated interface.

The density profiles show that the decane and water bulk phases have their own bulk density, indicating that the system size is fairly large enough to describe the interface between bulk phases. Using the 90−90 interface, the interfacial thickness of the bare decane−water interface is found to be in good agreement with experimental observation. It is also observed that the interface thickness of decane (t_{oil}) varies as a function

of the attachment position of benzene sulfonate, while the water interface was not affected by such structural variation. From such thickness analysis, we found that surfactant 4-C16 results in the maximum interfacial broadening effect among the surfactants, and the interfacial thickness decreases as the attachment position is located farther from the fourth carbon. The reason might be that the alkyl tail of 4-C16 has better miscibility with decane than the other surfactants since the interfacial thickness is broadened as the miscibility increases.

The interfacial tension profile was calculated along the *z*-axis direction (perpendicular to the interface) using the Kirkwood−Buff theory. In each bulk phase for decane and water, the interfacial tension profile showed a value of zero, indicating that the pressure difference ($P_N - P_T$) exists only at the interface because of the structural anisotropy. On the contrary, where the decane−water interface has a single peak, the surfactant-mediated interface has double peaks, which means that the actual interface consists of two subinterfaces at the molecular level: one for the decane−surfactant and the other for the surfactant−water. The values of interfacial tension were calculated by integrating the profiles along the *z*-axis direction. Through the comparison among the surfactants, we found that surfactant 4-C16 induces the lowest interfacial tension, and the IFT increases as the attachment position is located farther from the fourth carbon. Therefore, there is a correlation between the interfacial thickness and the interfacial tension: the interfacial tension decreases as the interfacial thickness (or the miscibility) increases.

To rationalize the difference in the miscibility of *m*-C16 with decane in terms of the size similarity, we introduced the effective length of the alkyl tail of each surfactant as the difference between the average length of the long tail and of the short tail and compared with the end-to-end length of decane. The effective length of the 4-C16 alkyl tail (9.53 ± 1.36 Å) was remarkably closer to that of decane (9.97 ± 1.03 Å) than to those of the other surfactants, which is consistent with the results from the density profile and the IFT profile.

Acknowledgment. This research was supported in part by the Department of Energy (DE-FC26-01BC15362, Paul West). The facilities of the Materials and Process Simulation Center used for these studies are supported by DURIP-ARO, DURIP-ONR, IBM-SUR, and NSF (MRI), and other support for the MSC comes from MURI-ARO, MURI-ONR, DOE, ONR, NSF-CSEM, NIH, General Motors, ChevronTexaco, Seiko-Epson, Beckman Institute, and Asahi Kasei.

References and Notes

(1) Myers, D. *Surfactant Science and Technology*; VCH: New York, 1946.
(2) Dickinson, E.; Euston, S. R.; Woskett, C. M. *Prog. Colloid Polym. Sci.* **1990**, *82*, 65.
(3) *Interfacial Phenomena in Petroleum Recovery*; Morrow, N. M., Ed.; Dekker: New York, 1991.
(4) *Liquid−Liquid Interface: Theory and Methods*; Volkov, A. G., Deamer, D. W., Eds.; CRC: Boca Raton, FL, 1996.
(5) Rosen, M. J.; Murphy, D. S. *Langmuir* **1991**, *7*, 2630.
(6) Liggieri, L.; Ravera, F.; Passerone, A. *J. Colloid Interface Sci.* **1995**, *169*, 238.
(7) Ferrari, M.; Liggieri, L.; Ravera, F.; Amodio, C.; Miller, R. *J. Colloid Interface Sci.* **1997**, *186*, 40.
(8) Hansen, F. K.; Fagerheim, H. *Colloids Surf., A* **1998**, *137*, 217.
(9) Kalinin, V. V.; Radke, C. J. *Colloids Surf., A* **1996**, *114*, 337.
(10) Vaughn, M. W.; Slattery, J. C. *J. Colloid Interface Sci.* **1997**, *195*, 1.
(11) Fainerman, V. B.; Miller, R.; Wuestneck, R.; Makievski, A. V. *J. Phys. Chem.* **1996**, *100*, 7669.
(12) Fainerman, V. B.; Miller, R.; Wuestneck, R. *J. Phys. Chem. B* **1997**, *101*, 6479.
(13) Fainerman, V. B.; Zholob, S. A.; Miller, R. *Langmuir* **1997**, *13*, 283.
(14) Fainerman, V. B.; Makievski, A. V.; Miller, R. *Rev. Chem. Eng.* **1998**, *14*, 373.
(15) Ravera, F.; Ferrari, M.; Liggieri, L.; Miller, R.; Passerone, A. *Langmuir* **1997**, *13*, 4817.
(16) Ravera, F.; Ferrari, M.; Liggieri, L. *Adv. Colloid Interface Sci.* **2000**, *88*, 129.
(17) Mulqueen, M.; Blankschtein, D. *Langmuir* **1999**, *15*, 8832.
(18) Mulqueen, M.; Blankschtein, D. *Langmuir* **2000**, *16*, 7640.
(19) Mulqueen, M.; Blankschtein, D. *Langmuir* **2002**, *18*, 365.
(20) Nikas, Y. J.; Puvvada, S.; Blankschtein, D. *Langmuir* **1992**, *8*, 2680.
(21) Freeman, K.-S. C.; McDonald, I. R. *Mol. Phys.* **1973**, *26*, 529.
(22) Liu, K. S. *J. Chem. Phys.* **1974**, *60*, 4226.
(23) Rao, M.; Levesque, D. *J. Chem. Phys.* **1976**, *65*, 3233.
(24) Miyazaki, J.; Barker, J. A.; Pound, G. M. *J. Chem. Phys.* **1976**, *64*, 3364.
(25) Rao, M.; Berne, B. J. *Mol. Phys.* **1979**, *37*, 455.
(26) Croxton, C. A. *Statistical Mechanics of the Liquid Surface*; Wiley: New York, 1980.
(27) Lee, C. Y.; Scott, H. L. *J. Chem. Phys.* **1980**, *73*, 4591.
(28) Townsend, R. M.; Gryko, J.; Rice, S. A. *J. Chem. Phys.* **1985**, *82*, 4391.
(29) Wilson, M. A.; Pohorille, A.; Pratt, L. R. *J. Phys. Chem.* **1987**, *91*, 4873.
(30) Brodskaya, E. N.; Rusanov, A. I. *Mol. Phys.* **1987**, *62*, 251.
(31) Matsumoto, M.; Kataoka, J. *J. Chem. Phys.* **1988**, *88*, 3233.
(32) Benjamin, I. *J. Chem. Phys.* **1991**, *94*, 662.
(33) Pohorille, A.; Benjamin, I. *J. Chem. Phys.* **1991**, *94*, 5599.
(34) Harris, J. G. *J. Phys. Chem.* **1992**, *96*, 5077.
(35) Linse, P. *J. Chem. Phys.* **1987**, *86*, 4177.
(36) Gao, J.; Jorgensen, W. L. *J. Phys. Chem.* **1988**, *92*, 5813.
(37) Smit, B. *Phys. Rev. A* **1988**, *37*, 3431.
(38) Meyer, M.; Mareschal, M.; Hayoun, M. *J. Chem. Phys.* **1988**, *89*, 1067.
(39) Carpenter, I. L.; Hehre, W. J. *J. Phys. Chem.* **1990**, *94*, 531.
(40) Smit, B.; Hilbers, P.-A. J.; Esselink, K.; Rupert, L.-A. M.; van Os, N. M.; Schlijper, A. G. *J. Phys. Chem.* **1991**, *95*, 6361.
(41) Benjamin, I. *J. Chem. Phys.* **1992**, *97*, 1432.
(42) van Buuren, A. R.; Marrink, S.-J.; Berendsen, H.-J. C. *J. Phys. Chem.* **1993**, *97*, 9206.
(43) Esselink, K.; Hilbers, P.-A. J.; van Os, N. M.; Smit, B.; Karaborni, S. *Colloids Surf., A* **1994**, *91*, 155.
(44) Zhang, Y.; Feller, S. E.; Brooks, B. R.; Pastor, R. W. *J. Chem. Phys.* **1995**, *103*, 10252.
(45) Michael, D.; Benjamin, I. *J. Phys. Chem.* **1995**, *99*, 1530.
(46) Benjamin, I. *Annu. Rev. Phys. Chem.* **1997**, *48*, 407.
(47) Panhuis, M.-I. H.; Karaborni, S. *Philos. Mag. B* **1999**, *79*, 9.
(48) Diaz-Herrera, E.; Alejandre, J.; Ramirez-Santiago, G.; Forstmann, F. *J. Chem. Phys.* **1999**, *110*, 8084.
(49) Kuhn, H.; Rehage, H. *Colloid Polym. Sci.* **2000**, *278*, 114.
(50) Nicolas, J. P. *Biophys. J.* **2003**, *85*, 1377.
(51) Rivera, J. L.; McCabe, C.; Cummings, P. T. *Phys. Rev. E* **2003**, *67*, 011603.
(52) Karaborni, S.; Esselink, K.; Hilbers, P.-A. J.; Smit, B.; Karthauser, J.; van Os, N. M.; Zana, R. *Science* **1994**, *266*, 254.
(53) Maiti, P. K.; Chowdhury, D. *Europhys. Lett.* **1998**, *41*, 183.
(54) Maiti, P. K.; Chowdhury, D. *J. Chem. Phys.* **1998**, *109*, 5126.
(55) Maiti, P. K.; Kremer, K.; Flimm, O.; Chowdhury, D.; Stauffer, D. *Langmuir* **2000**, *16*, 3784.
(56) Maiti, P. K.; Lansac, Y.; Glaser, M. A.; Clark, N. A.; Rouault, Y. *Langmuir* **2002**, *18*, 1908.
(57) Doe, P. H.; Wade, W. H.; Schechter, R. S. *J. Colloid Interface Sci.* **1977**, *59*, 525.
(58) Siepmann, J. I.; Karaborni, S.; Smit, B. *Nature* **1993**, *365*, 330.
(59) Smit, B.; Karaborni, S.; Siepmann, J. I. *J. Chem. Phys.* **1995**, *102*, 2126.
(60) Martin, M. G.; Siepmann, J. I. *J. Am. Chem. Soc.* **1997**, *119*, 8921.
(61) Nicolas, J. P.; Smit, B. *Mol. Phys.* **2002**, *100*, 2471.
(62) Levitt, M.; Hirshberg, M.; Sharon, R.; Laidig, K. E.; Daggett, V. *J. Phys. Chem. B* **1997**, *101*, 5051.
(63) Jang, S. S.; Cagin, T.; Goddard, W. A., III *J. Chem. Phys.* **2003**, *119*, 1843.
(64) Jang, S. S.; Molinero, V.; Cagin, T.; Goddard, W. A., III *J. Phys. Chem. B* **2004**, *108*, 3149.
(65) Mayo, S. L.; Olafson, B. D.; Goddard, W. A., III *J. Phys. Chem.* **1990**, *94*, 8897.
(66) Calvo, E.; Brocos, P.; Bravo, R.; Pintos, M.; Amigo, A.; Roux, A. H.; Roux-Desgranges, G. *J. Chem. Eng. Data* **1998**, *43*, 105.
(67) Sastry, N. V.; Valand, M. K. *J. Chem. Thermodyn.* **1998**, *30*, 929.
(68) Trenzado, J. L.; Matos, J. S.; Segade, L.; Carballo, E. *J. Chem. Eng. Data* **2001**, *46*, 974.

(69) Bjola, B. S.; Siddiqi, M. A.; Fornefeld-Schwarz, U.; Svejda, P. *J. Chem. Eng. Data* **2002**, *47*, 250.
(70) Kell, G. S.; Haar, L.; Gallagher, J. S. *NBS/NRC Steam Tables*; Hemisphere Publishing Corp.: Washington, DC, 1984.
(71) Pai, Y. H.; Chen, L. J. *J. Chem. Eng. Data* **1998**, *43*, 665.
(72) Tsierkezos, N. G.; Molinou, I. E. *J. Chem. Eng. Data* **1998**, *43*, 989.
(73) Plimpton, S. J. *J. Comput. Phys.* **1995**, *117*, 1.
(74) Plimpton, S. J.; Pollock, R.; Stevens, M. The Eighth SIAM Conference on Parallel Processing for Scientific Computing; Minneapolis, MN, 1997.
(75) Verlet, L. *Phys. Rev.* **1967**, *159*, 98.
(76) Nose, S.; Klein, M. L. *J. Chem. Phys.* **1983**, *78*, 6928−6939.
(77) Nose, S. *J. Chem. Phys.* **1984**, *81*, 511−519.
(78) Hoover, W. G. *Phys. Rev. A* **1985**, *31*, 1695.
(79) Melchionna, S.; Ciccotti, G.; Holian, B. L. *Mol. Phys.* **1993**, *78*, 533.
(80) Hockney, R. W.; Eastwood, J. W. *Computer Simulation using Particles*; McGraw-Hill: New York, 1981.
(81) Yoshida, T.; Taga, K.; Okabayashi, H.; Matsushita, K.; Kamaya, H.; Ueda, I. *J. Colloid Interface Sci.* **1986**, *109*, 336.
(82) Chapela, G. A.; Saville, G.; Thompson, S. M.; Rowlinson, J. S. *J. Chem. Soc., Faraday Trans. 2* **1977**, *73*, 1133−1144.
(83) Walton, J. P. R. B.; Tildesley, D. J.; Rowlinson, J. S.; Henderson, J. R. *Mol. Phys.* **1983**, *48*, 1357.
(84) Alejandre, J.; Tildesley, D. J.; Chapela, G. A. *J. Chem. Phys.* **1995**, *102*, 4574.
(85) Rivera, J. L.; Predota, M.; Chialvo, A. A.; Cummings, P. T. *Chem. Phys. Lett.* **2002**, *357*, 189.
(86) Mitrinovic, D. M.; Tikhonov, A. M.; Li, M.; Huang, Z.; Schlossman, M. L. *Phys. Rev. Lett.* **2000**, *85*, 582.
(87) Ono, S.; Kondo, S. In *Encyclopedia of Physics*; Flugge, S., Ed.; Springer: Berlin, 1960; Vol. 10.
(88) Hill, T. L. *Introduction to Statistical Mechanics*; Dover: New York, 1986.
(89) Kirkwood, J. G.; Buff, F. P. *J. Chem. Phys.* **1949**, *17*, 338.
(90) Chen, L.-J. *J. Chem. Phys.* **1995**, *103*, 10214.
(91) Jasper, J. J. *J. Phys. Chem. Ref. Data* **1972**, *1*, 841.
(92) Alvarez, E.; Rendo, R.; Sanjurjo, B.; Sanchez-Vilas, M.; Navaza, J. M. *J. Chem. Eng. Data* **1998**, *43*, 1027−1029.
(93) Zeppieri, S.; Rodriguez, J.; de Ramos, A.-L. L. *J. Chem. Eng. Data* **2001**, *46*, 1086.